

# On the Calculation and Modeling of Magnetic Exchange Interactions in Weakly Bonded Systems: The Case of the Ferromagnetic Copper(II) $\mu_2$ -Azido Bridged Complexes

**Carlo Adamo**

Dipartimento di Chimica, Università della Basilicata, Potenza, Italy

**Vincenzo Barone**

Dipartimento di Chimica, Università di Napoli, Napoli, Italy

**Alessandro Bencini\* and Federico Totti**

Dipartimento di Chimica, Università di Firenze, Firenze, Italy

**Ilaria Ciofini**

Institute of Inorganic and Analytical Chemistry, University of Fribourg, Fribourg, Switzerland

Received October 19, 1998

The magnetic exchange interactions in copper(II)  $\mu_2$ -azido bridged complexes have been studied using several density functionals and both GTO and STO basis sets. From a methodological point of view, we have taken into proper account nonorthogonality effects in the framework of the broken symmetry approach. A remarkable agreement with experimental data has been obtained using the crystallographic geometry and the new MPW1PW functional. However, modeling of the true ligands by ammonia molecules and complete optimization of the geometry of the isolated complex significantly deteriorate the results. While this can lead to limitations on quantitative studies, general trends and magnetostructural correlations remain very significant. These results are, furthermore, not very sensitive to technical details, like the form of the functional or the type of basis set used.

## Introduction

The calculation of the magnetic structure of binuclear transition metal complexes or organic biradicals has known a renewed interest among computational chemists in the last years.<sup>1</sup> This is mainly due to the fundamental role which a deeper understanding of the phenomena which govern spin correlation in dimers played in many areas of research, ranging from bioinorganic<sup>2</sup> to solid-state chemistry.<sup>3</sup> The magnetic properties of molecular solids are governed by nearest neigh-

bor's interactions, which are present in the simplest binuclear moieties. These are now qualitatively rather well understood, within the "active electron approximation", on the basis of the overlap between magnetic orbitals (super-exchange) and spin-polarization mechanisms.<sup>4,5</sup> These effects also lead to the onset of the bulk properties of magnetic materials when modulated by less strong long-range interactions between molecules in the same unit cell.<sup>6</sup> The proper description of the long range interactions is another challenging field in theoretical magnetism.<sup>1k</sup>

Binuclear complexes of transition metal ions or organic biradicals most often present a large variability in the spin of the ground electronic state as a consequence of small geometric deformations.<sup>7</sup> The environment, rather than electronic factors, often modulates the geometry of the actual compounds and makes modeling of the magnetic properties cumbersome if based on geometries optimized on the isolated molecules in the gas phase.

- (1) (a) Miralles, J.; Daudey, J. P.; Caballol, R. *Chem. Phys. Lett.* **1992**, *198*, 555. (b) Miralles, J.; Castell, O.; Caballol, R.; Malrieu, J. P. *Chem. Phys.* **1993**, *172*, 33. (c) Castell, O.; Miralles, J.; Caballol, R. *J. P. Chem. Phys.* **1994**, *179*, 377. (d) Fink, K.; Fink, R.; Staemmler, V. *Inorg. Chem.* **1994**, *33*, 6219. (e) Ovcharenko, V. I.; Romanenko, G. V.; Ikorskii, V. N.; Musin, R. N.; Sagdeev, R. Z. *Inorg. Chem.* **1994**, *33*, 3370. (f) Wang, C.; Fink, K.; Staemmler, V. *Chem. Phys.* **1995**, *201*, 87. (g) Noodleman, L.; Peng, C. Y.; Case, D. A.; Mouesca, J. M. *Coord. Chem. Rev.* **1995**, *144*, 199. (h) Bencini, A.; Totti, F.; Daul, C.; Doclo, K.; Fantucci, P.; Barone, V. *Inorg. Chem.* **1997**, *36*, 5022. (i) Caballol, R.; Castell, O.; Illas, F.; Moreira, P. R.; Malrieu, J. P. *J. Phys. Chem.* **1997**, *101*, 7860. (j) Barone, V.; Bencini, A.; Di Matteo, A. *J. Am. Chem. Soc.* **1997**, *119*, 10831. (k) Barone, V.; Bencini, A.; Cossi, M.; Di Matteo, A.; Mattesini, M.; Totti, F. *J. Am. Chem. Soc.* **1998**, *120*, 7069.
- (2) (a) Sauer, K. *Acc. Chem. Res.* **1980**, *13*, 249. (b) *Iron–Sulfur Proteins*; Spiro, T. G., Ed.; Wiley and Sons: New York, 1982. (c) *Iron–Sulfur Proteins*; Cammack, R., Ed.; Adv. Inorg. Chem. 38; Academic Press: San Diego, 1992. (d) Barber, J. *Nature* **1995**, *376*, 388.
- (3) (a) Gatteschi, D. *Adv. Mater.* **1994**, *6*, 635. (b) Miller, J. S.; Epstein, A. *J. Angew. Chem., Int. Ed. Engl.* **1994**, *33*, 385.

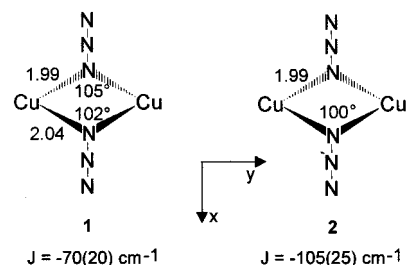
- (4) (a) Hay, P. J.; Thibault, J. C.; Hoffmann, R. *J. Am. Chem. Soc.* **1975**, *97*, 4884. (b) Kahn, O.; Briat, B. *J. Chem. Soc., Faraday Trans. 2* **1976**, *72*, 268.
- (5) Kahn, O. *Molecular Magnetism*; VCH: New York, 1993.
- (6) Slater, J. C. *Quantum Theory of Molecules and Solids. Vol. 4: Self-Consistent Field for Molecules and Solids*; McGraw-Hill: New York, 1974.
- (7) (a) *Magneto Structural Correlations in Exchange Coupled Systems*; Willett, R. D., Gatteschi, D., Kahn, O., Eds.; NATO Adv. Studies Ser. C Reidel: Dordrecht, 1985. (b) *Magnetic Molecular Materials*; Gatteschi, D., Kahn, O., Miller, J. S., Palacio, F., Eds.; NATO Adv. Studies Ser.; Reidel: Dordrecht, 1985.

The simplest systems to be investigated theoretically are those containing only two active electrons. The ground state can be either a triplet ( $S = 1$ ) or a singlet ( $S = 0$ ) and the separation between these two levels, which arises from weak bonding interactions, can range from a few to some hundreds of wavenumbers. Calculation of the singlet–triplet separation in these systems requires therefore an *ab initio* computational approach that could handle large molecular systems. We have recently computed the singlet–triplet splitting in a number of model complexes.<sup>1h</sup> Different approaches were compared, based on density functional theory (DFT),<sup>8</sup> the most widely applied tool for the investigation of the electronic structure and properties of large molecules and solids.<sup>9</sup> In most cases, the broken symmetry (BS) approach, developed by Noodleman et al.,<sup>10</sup> was found to give accurate results. This formalism, which was developed in order to avoid the use of extensive post-Hartree–Fock corrections to the energies of the spin multiplets, is based on an unrestricted SCF calculation of a broken symmetry wave function. This wave function is formed by one Slater determinant built up using molecular orbitals localized onto the two paramagnetic centers and bearing opposite spins. This determinant is not an eigenstate of  $S^2$ , but corresponds to a total  $M_s = 0$  state or, more generally, to the minimum  $M_s$  value. The energy of this state (the BS state) contains the most important contributions to the singlet–triplet separation, including the ligand bridge effects often called *ligand spin polarization*.<sup>10c</sup> The singlet–triplet separation,  $E_S - E_T$ , can be easily computed from the energy of the BS state,  $E_{BS}$ , and that of the triplet state,  $E_T$ , under the assumption that spin contamination of the triplet state from higher spin states is negligible, by

$$E_S - E_T = 2[E_{BS} - E_T] \quad (1)$$

$E_S - E_T$  is most often experimentally obtained from magnetic measurements as  $J$ , the magnetic coupling constant, which, if one uses the spin Hamiltonian in the form  $H = J(S_1 \cdot S_2)$ , is defined by  $J = -(E_S - E_T)$ .<sup>5,11</sup> A positive value of  $J$  determines a singlet ground state. In this case, the magnetic interaction between the paramagnetic centers is called antiferromagnetic interaction. The highest occupied molecular orbitals issuing from BS calculation<sup>5</sup> are localized and nonorthogonal; these are usually a good description of the *natural magnetic orbitals*, used for a chemical understanding of the magnetic exchange interactions in terms of exchange pathways.<sup>5</sup> Equation 1 has been widely used to compute  $J$  in a variety of systems,<sup>1a–c, h–k</sup> but it is strictly valid only when the square of the overlap between the magnetic orbitals is much smaller than 1, a situation which can be met in weakly coupled systems. In the case of strong overlap, the magnetic orbitals are no longer localized, but are close the symmetric molecular orbitals corresponding to their in-phase and out-of-phase linear combinations.<sup>10,12</sup> In this limiting case, the BS state is close to the lowest singlet state and eq 1 becomes  $E_S - E_T = [E_{BS} - E_T]$ . Recently the energy of the BS state was assumed to be the energy of the pure singlet

## Scheme 1



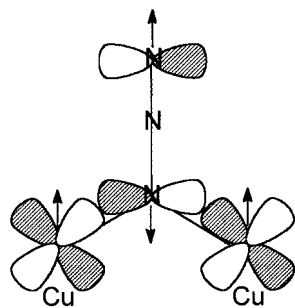
state even in weakly bonded systems.<sup>13</sup> All the correlation effects were claimed to be included in the functional used, namely B3LYP.<sup>14</sup> Since, however, in the weak bonding situation, the BS wave function is build up by orbitals with different spatial extension, say  $a$  and  $b$ , the real singlet state is a multideterminant function and cannot be represented by the Slater determinant  $|a^+b^-|$  which is the BS wave function. We therefore will not use this approach in the present paper, but we will apply a spin projection technique to obtain the energy of the pure singlet from that of the BS state. This procedure can lead to an overestimation of the correlation of the singlet state, which is partially included in the use of localized orbitals in the BS determinant and in the functional of the density. For this reason, the effect of the form of the functional on the computed  $J$  values will be also investigated.

In the field of molecular magnetism it has been recognized for several years that azido ion,  $N_3^-$ , when bridging two paramagnetic metal ions in the  $\mu$ -1,1 or end-on mode, stabilizes a ferromagnetic interaction between them.<sup>5,15</sup> Two classical examples of such complexes are the two bis( $\mu$ -1,1-azido) bridged copper(II) complexes:  $[Cu_2(N_3)_4([24]ane-N_2O_6)1 \cdot H_2O]$  (**1**) ( $[24]ane = C_{16}H_{34}N_2O_6$ ) and  $[Cu_2(tbupy)_4(N_3)_2](ClO_4)_2$  (**2**) ( $tbupy = tert$ -butylpyridine).<sup>16</sup> The geometry of the bridging groups and the measured  $J$  values of the above-mentioned complexes are shown in the Scheme 1. While the structure of the bridging group is similar in the two complexes, they largely differ in the nature of the terminal ligand, a criptand macrocycle in **1** with a distorted octahedral coordination of copper(II) and a substituted pyridine in **2** with copper(II) in a square planar coordination. In any case, however, the magnetic orbitals are formed mainly by  $3d(xy)$  metal orbitals. Kahn et al., using the polarization of the spin of the electrons in the magnetic orbitals, rationalized the ferromagnetism of these molecules.<sup>17</sup> This mechanism of magnetic exchange is pictorially shown in Scheme 2. It was shown that this effect is accounted for by configuration interaction in a molecular orbital picture.<sup>17</sup> Recently, the magnetic and spectroscopic properties of **2** have been interpreted using a valence bond configuration interaction model, which parametrizes the magnetic interactions in terms of charge-transfer transitions.<sup>18</sup> In this last paper, the main configuration which contributes to the stabilization of the triplet state was found to be a mixing of the triplet state which is

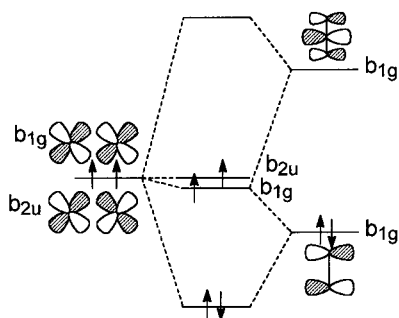
- (8) Parr, R. G.; Young, W. *Density Functional Theory of Atoms and Molecules*; Oxford University Press: New York, 1989.  
 (9) (a) St-Amant, A. In *Density Functional Methods in Biomolecular Modeling*; Lipkowitz, K. B., Boyd, D. B., Eds.; VCH Publisher: New York, 1996. (b) Singh, D. *Plane waves, pseudopotentials and the LAPW method*; Kluwer Academic: Norwell, MA, 1994.  
 (10) (a) Noodleman, L.; Norman, J. G., Jr. *J. Chem. Phys.* **1979**, *70*, 4903. (b) Noodleman, L. *J. Chem. Phys.* **1981**, *74*, 5737. (c) Noodleman, L.; Davidson, E. R. *Chem. Phys.* **1986**, *109*, 131.  
 (11) Bencini, A.; Gatteschi, D. *EPR of Exchange Coupled Systems*; Springer-Verlag: Heidelberg, 1990.  
 (12) Albonico, C.; Bencini, A. *Inorg. Chem.* **1988**, *27*, 1934.

- (13) Riuz, E.; Cano, J.; Alvarez, S.; Alemany, P. *J. Am. Chem. Soc.* **1998**, *120*, 11122.  
 (14) Becke, A. D. *J. Chem. Phys.* **1993**, *98*, 5648.  
 (15) (a) Vicente, R.; Escuer, A.; Ribas, J.; Salah el Fallah, M.; Solans, X.; Font-Bardia, M. *Inorg. Chem.* **1993**, *32*, 1920. (b) Escuer, A.; Vicente, R.; Goher, M. A. S.; Mautner, F. A. *Inorg. Chem.* **1996**, *35*, 6386.  
 (16) (a) Comarmond, J.; Plumeré, P.; Lehn, J. M.; Agnus, Y.; Louis, R.; Weiss, R.; Kahn, O.; Morgestern-Badarau, I. *J. Am. Chem. Soc.* **1982**, *104*, 6330. (b) Sikorav, S.; Bkouche-Waksman, I.; Kahn, O. *Inorg. Chem.* **1984**, *23*, 490.  
 (17) Charlot, M.-F.; Kahn, O.; Chaillet, M.; Larrieu, C. *J. Am. Chem. Soc.* **1986**, *108*, 2574.  
 (18) von Seggern, I.; Tucek, F.; Bensch, W. *Inorg. Chem.* **1995**, *34*, 5530.

Scheme 2



Scheme 3



obtained by a single excitation to the LUMO of the  $N_3^-$  ligand. In terms of orbital interactions this corresponds to a  $\pi$ -anti-bonding interaction between the  $3d(xy)$  orbitals of the copper(II) ions and the LUMOs of  $N_3^-$ , as shown in Scheme 3. It is still an open question whether the spin polarization model accounts for the main part of the ferromagnetic interaction in the  $\mu$ -1,1-azido bridged copper(II) dimers or also other electronic effects, e.g., the so-called *super-exchange* mechanisms, are present. It is commonly accepted that geometrical dependency of  $J$  on geometrical factors is caused by these latter mechanisms. Since this dependence was never observed in doubly bridged end-on azido complexes it was concluded that the preferred mechanism for exchange interaction was spin polarization. A recent polarized neutron diffraction study was performed on **2**<sup>19</sup> whose results indicate that a significant spin delocalization is present over the whole molecule, which favors the presence of super-exchange mechanisms.

Methods of calculation based on the density functional theory were found to be a powerful tool for the understanding of the magnetic properties in a variety of systems.<sup>h,20</sup> Unfortunately, the exchange mechanisms, which have meaning in *ab initio* CI calculations,<sup>5</sup> cannot be separately computed in DFT, where state energies can only be computed. However, a computed dependence of  $J$  from structural parameters, which are expected not severely alter spin polarization effects, can be used to evidence the possible role of super-exchange interactions.

Beside the chemical problem, which we are addressing with DFT, we will also test, in this paper, the validity of the approaches commonly used in the calculation of  $J$ . The following points, which have large interest for theoretical magnetochemists, will be considered.

(a) The dependence of the  $J$  values on the form of the density functional, and on the basis function type, namely, Gaussian-type orbitals (GTO) or Slater-type orbitals (STO) will be studied. The influence of the functional form on the computed  $J$  values will be explored by comparing the results obtained with various functionals, including the hybrid HF/DF models like the popular B3LYP<sup>21</sup> and the recently developed MPW1PW.<sup>22</sup> This latter functional has been applied with the same performances of the B3LYP one in a number of cases ranging from covalently bonded systems to noncovalent interactions and activation barriers,<sup>22</sup> and it will be used here to calculating the magnetic structure of ferromagnetic copper(II) dimers. Some comparison between the results obtained by using STO and GTO bases will also be made. In this way we offer a comparison as extensive as possible between two of the most widely used density functional computer codes.

(b) The results obtained using (1) will be compared with those obtained by a procedure recently suggested by Ovchinnikov and Labanowski<sup>23</sup> for computing the pure singlet energies from unrestricted Hartree–Fock or DFT calculations.

(c) The influence of the actual model molecule used in the calculation will be exploited. A common procedure, when computing magnetic observables, is to perform calculations on model complexes whose structure averages the molecular structures found in a series of complexes with the same bridging moieties. In general, they have different terminal ligands, which are modeled by molecular groups smaller than the real ligands. This procedure is based on the assumption that the nature of the terminal ligand only slightly alters the overall  $J$  values. In the present calculations, we used ammonia molecules as terminal model ligands, as well as pyridines, which are closer to the *tert*-butylpyridine ligand of complex **2**. The results we obtained show that the nature of the terminal ligands is extremely important in order to obtain a value of  $J$  closer to the experimental findings.

(d) Magnetostructural correlations will be established: “The real test of understanding is prediction.”<sup>24</sup> The computed dependence of  $J$  on structural parameters leads to an unprecedented antiferromagnetic behavior of the double end-on azido bridging ligand and constitutes a challenge for more synthetic work. As a matter of fact, no copper(II) compound with double end-on  $N_3^-$  ions was found to be antiferromagnetic. Antiferromagnetism has been observed only in some compound containing other ligands together with  $N_3^-$ .<sup>25</sup>

In the following, the paper will be divided into a section briefly reviewing the spin projection technique used, a section presenting the computational details, and a final part with the results and the computed magneto-structural correlations.

### Spin Projection Technique

As already shown in ref 10, the BS wave function,  $\Psi_{BS}$ , is a linear combination of a pure singlet,  $\Psi_0$ , and a pure triplet wave function,  $\Psi_1$ . We can therefore write, in the general case,<sup>23</sup>

$$\Psi_{BS} = a_0\Psi_0 + a_1\Psi_1 \quad (2)$$

with

(19) Aebersold, M. A.; Gillon, B.; Plantevin, O.; Pardi, L.; Kahn, O.; Bergerat, P.; von Seggern, I.; Tuzek, F.; Öhrström, L.; Grand, A.; Lelièvre-Berna, E. *J. Am. Chem. Soc.* **1998**, *120*, 5238.  
 (20) (a) Bencini, A. *J. Chem. Phys.* **1989**, *86*, 763. (b) Bencini, A.; Ghilardi, C. A.; Orlandini, A.; Midollini, S.; Zanchini, C. *J. Am. Chem. Soc.* **1992**, *114*, 8989. (c) Bencini, A.; Midollini, S. *Coord. Chem. Rev.* **1992**, *120*, 87. (d) Bencini, A.; Uytterhoeven, M. G.; Zanchini, C. *Int. J. Quantum. Chem.* **1994**, *52*, 903

(21) (a) Becke, A. D. *J. Chem. Phys.* **1993**, *98*, 5648. (b) Stephens, P. J.; Devlin, F. J.; Frisch, M. J.; Chabalowski, C. F. *J. Phys. Chem.* **1994**, *98*, 11623.  
 (22) Adamo, C.; Barone, V. *J. Chem. Phys.* **1998**, *108*, 627.  
 (23) Ovchinnikov, A.; Labanowski, J. K. *Phys. Rev.* **1996**, *A53*, 3946.  
 (24) Hoffmann, R. *Solids and Surfaces*; VCH: New York, 1988.  
 (25) Thompson, L. K.; Tandon, S. S. *Comments Inorg. Chem.* **1996**, *18*, 125.



**Table 1.** Computed Values of  $J$  and  $J_{\text{cor}}$  ( $\text{cm}^{-1}$ ) for  $[(\text{NH}_3)_2\text{Cu}(\mu\text{-}1,1\text{-N}_3)_2\text{Cu}(\text{NH}_3)_2]^{2+}$  at Various Values of  $r$  and  $\varphi$  with Different Functionals<sup>a</sup>

method <sup>b</sup>		$\varphi$ (deg)				
		86	90	96	100	106
$r = 2.2 \text{ \AA}$						
HF	$J_{\text{cor}}$	-512.3	-534.4	-536.0	-516.3	-458.0
	$J$	-509.2	-531.2	-533.0	-513.4	-455.3
	$S^2$	1.0061	1.0059	1.0057	1.0057	1.0057
X $\alpha$	$J_{\text{cor}}$	1402.0	1627.1	2024.6	2305.5	2705.8
	$J$	1819.6	2157.4	2798.8	3292.0	4068.2
	$S^2$	0.7021	0.6741	0.6176	0.5721	0.4965
VWN	$J_{\text{cor}}$	1758.7	1982.7	2373.5	2645.1	3024.8
	$J$	2440.6	2826.2	3563.6	4133.0	5033.8
	$S^2$	0.6213	0.5746	0.4986	0.4375	0.3358
B3LYP	$J_{\text{cor}}$	287.9	456.9	782.7	1037.2	1452.2
	$J$	305.2	487.0	844.0	1129.3	1609.0
	$S^2$	0.9400	0.9342	0.9217	0.9111	0.8920
B3PW91	$J_{\text{cor}}$	267.4	435.1	757.5	1008.6	1417.0
	$J$	282.9	463.0	815.4	1096.2	1566.5
	$S^2$	0.9417	0.9359	0.9236	0.9132	0.8946
MPW1PW	$J_{\text{cor}}$	24.0	435.1	860.5	683.7	1417.0
	$J$	25.4	463.0	926.2	722.8	1566.5
	$S^2$	0.9417	0.9359	0.9236	0.9428	0.8946
$r = 2.1 \text{ \AA}$						
HF	$J_{\text{cor}}$	-584.7	-625.7	-646.7	-632.6	-571.0
	$J$	-581.0	-621.9	-642.8	-628.8	-567.6
	$S^2$	1.0064	1.0063	1.0061	1.0060	1.0059
X $\alpha$	$J_{\text{cor}}$	911.4	1145.4	1578.3	1890.8	2334.5
	$J$	1107.8	1423.8	2052.8	2547.6	3327.2
	$S^2$	0.7845	0.7569	0.6994	0.6526	0.5748
VWN	$J_{\text{cor}}$	1237.5	1476.9	1913.9	2223.4	2654.4
	$J$	1585.2	1946.8	2671.2	3243.8	4125.0
	$S^2$	0.7190	0.6818	0.6043	0.5411	0.4358
B3LYP	$J_{\text{cor}}$	-52.4	105.9	428.6	687.7	1113.2
	$J$	-54.3	110.6	452.8	733.6	1207.8
	$S^2$	0.9619	0.9560	0.9436	0.9333	0.9150
B3PW91	$J_{\text{cor}}$	-68.1	89.2	408.9	664.8	1083.9
	$J$	-70.6	93.0	431.5	708.3	1174.0
	$S^2$	0.9629	0.9571	0.9449	0.9348	0.9169
MPW1PW	$J_{\text{cor}}$	-245.3	-125.7	163.9	390.8	771.6
	$J$	-250.6	-129.0	169.6	407.5	814.6
	$S^2$	0.9785	0.9741	0.9651	0.9576	0.9443
$r = 2.0 \text{ \AA}$						
HF	$J_{\text{cor}}$	-671.2	-738.2	-799.7	-801.0	-742.8
	$J$	-666.6	-738.2	-794.4	-794.2	-738.0
	$S^2$	1.0069	1.0000	1.0066	1.0085	1.0064
X $\alpha$	$J_{\text{cor}}$	340.4	563.4	1004.0	1333.6	1804.7
	$J$	386.4	653.6	1218.6	1678.4	2405.0
	$S^2$	0.8649	0.8399	0.7862	0.7415	0.6674
VWN	$J_{\text{cor}}$	622.1	858.0	1317.2	1655.0	2127.2
	$J$	731.0	1036.6	1686.6	2218.8	3066.2
	$S^2$	0.8250	0.7918	0.7196	0.6593	0.5586
B3LYP	$J_{\text{cor}}$	-399.3	-265.7	31.4	281.6	699.1
	$J$	-407.6	-272.6	32.6	295.0	744.2
	$S^2$	0.9793	0.9739	0.9623	0.9525	0.9355
B3PW91	$J_{\text{cor}}$	-412.1	-279.3	15.7	263.2	674.9
	$J$	-420.4	-286.4	16.0	275.4	717.6
	$S^2$	0.9798	0.9745	0.9818	0.9535	0.9368
MPW1PW	$J_{\text{cor}}$	-530.9	-423.5	-172.8	44.8	422.1
	$J$	-536.4	-429.6	-176.8	45.8	440.0
	$S^2$	0.9897	0.9857	0.9773	0.9702	0.9577
ADF-X $\alpha$	$J$	269.8	538.0	1128.6	1633.0	2481.8
ADF-VWN-Stoll	$J$	481.6	775.4	1430.4	1996.6	2953.3
$r = 1.9 \text{ \AA}$						
HF	$J_{\text{cor}}$	-763.7	-885.6	-1004.7	-1033.0	-998.0
	$J$	-758.0	-879.0	-997.2	-1025.6	-991.0
	$S^2$	1.0075	1.0073	1.0075	1.0072	1.0070
X $\alpha$	$J_{\text{cor}}$	-262.5	-88.4	299.9	612.0	1065.8
	$J$	-279.0	-95.6	337.6	712.0	1306.4
	$S^2$	0.9370	0.9180	0.8744	0.8366	0.7742
VWN	$J_{\text{cor}}$	-35.9	154.7	574.0	906.1	1381.1
	$J$	-38.8	170.8	667.0	1098.6	1790.6
	$S^2$	0.9878	0.9763	0.9435	0.9113	0.8572
B3LYP	$J_{\text{cor}}$	-738.6	-651.8	-416.0	-197.3	189.3
	$J$	-743.7	-659.2	-424.8	-203.2	187.8
	$S^2$	0.9930	0.9886	0.9788	0.9702	0.9552

Table 1 (Continued)

method <sup>b</sup>		$\varphi$ (deg)				
		86	90	96	100	106
				$r = 1.9 \text{ \AA}$		
B3PW91	$J_{\text{cor}}$	-750.4	-703.4	-429.5	-212.8	159.8
	$J$	-755.4	-671.2	-438.4	-219.0	166.8
	$S^2$	0.9933	0.9889	0.9792	0.9708	0.9561
MPW1PW	$J_{\text{cor}}$	-816.8	-754.5	-561.6	-373.8	-38.1
	$J$	-818.0	-758.0	-568.2	-380.6	-38.9
	$S^2$	0.9986	0.9954	0.9888	0.9819	0.9708
				$r = 1.8 \text{ \AA}$		
HF	$J_{\text{cor}}$	-840.7	-1042.2	-1267.1	-1351.0	-1369.7
	$J$	-835.4	-1033.6	-1256.6	-1339.8	-1358.6
	$S^2$	1.0063	1.0083	1.0083	1.0083	1.0081
X $\alpha$	$J_{\text{cor}}$	-766.9	-695.6	-464.8	-242.0	+99.6
	$J$	-775.0	-709.6	-486.2	-259.1	+110.8
	$S^2$	0.9895	0.9799	0.9539	0.9289	0.8876
VWN	$J_{\text{cor}}$	-575.4	-494.7	-239.1	+6.6	+382.7
	$J$	-582.4	-506.4	-252.6	+7.2	+437.4
	$S^2$	0.9878	0.9763	0.9435	0.9113	0.8572
B3LYP	$J_{\text{cor}}$	-1030.9	-1020.2	-900.0	-750.8	-467.3
	$J$	-1028.2	-1020.2	-906.0	-760.6	-478.8
	$S^2$	1.0026	1.0000	0.9934	0.9870	0.9755
B3PW91	$J_{\text{cor}}$	-1043.4	-1033.0	-913.2	-764.8	-484.6
	$J$	-1040.6	-1032.8	-919.0	-774.6	-496.2
	$S^2$	1.0027	1.0002	0.9886	0.9872	0.9760
MPW1PW	$J_{\text{cor}}$	-1070.4	-1080.5	-995.4	-870.9	-619.0
	$J$	-1065.4	-1077.4	-997.4	-876.8	-628.6
	$S^2$	1.0047	1.0029	0.9980	0.9932	0.9845

<sup>a</sup> When nonexplicitly indicated, the calculations were performed with GAUSSIAN94. <sup>b</sup> HF refers to broken symmetry calculations performed using the Hartree–Fock theory. The other symbols are the different functionals used in DFT (see text).

pseudopotentials. Calculations with ADF were performed using STO basis sets for  $r = 2.00 \text{ \AA}$  and  $\varphi$  in the range  $86^\circ$ – $106^\circ$ . The functionals used were the X $\alpha$ <sup>6</sup> and the VWN<sup>29</sup> ones. The Stoll correlation correction<sup>33</sup> for the electrons with the same spin was also used. The frozen core (FC) approximation for the inner core electrons was used. The orbitals up to 2p for copper and 1s for nitrogen were kept frozen. Double- $\zeta$  basis functions were applied to 3s and 3p valence orbitals of copper, to 2s and 2p orbitals of nitrogen, and to the 1s orbital of hydrogen. The 3d and 4p orbitals of copper were treated with triple- $\zeta$  and single- $\zeta$  functions, respectively. A 3d single- $\zeta$  polarization function was added to the nitrogen basis. The exponents of the Slater functions given with the ADF2.3 distribution were used throughout.

$J$  values computed through eqs 1 and 6,  $J$  and  $J_{\text{cor}}$ , respectively, were computed with GAUSSIAN94. Since, within the ADF package, the calculation of the expectation value of  $S^2$  is not yet implemented, only  $J$  was computed with ADF.

## Results and Discussion

The dependence of the  $J_{\text{cor}}$  values computed at  $r = 2.0 \text{ \AA}$  and by varying the  $\varphi$  angle for the model complex  $[(\text{NH}_3)_2\text{Cu}(\mu-1,1-\text{N}_3)_2\text{Cu}(\text{NH}_3)_2]^{2+}$  is graphically shown in Figure 2. Figure 3 shows the computed dependence of  $J_{\text{cor}}$  on  $r$ , while keeping  $\varphi = 100^\circ$ . More complete results are reported in Table 1. The calculations performed using STO's are also shown. In Table 1, both  $J$  and  $J_{\text{cor}}$  are reported together with the computed expectation value of  $S^2$ ,  $\langle S^2 \rangle$ , for the BS state. The values of  $\langle S^2 \rangle$  computed for the  $S = 1$  state are all in the range 2.00–2.01 independently on the functional in use. Significantly larger values (2.17–2.20) were computed using the Hartree–Fock method, indicating a significant contamination of the unrestricted triplet wave function, a well-known effect.<sup>34</sup> On the other hand, the pure local density functionals (X $\alpha$  and VWN) show a quite strong contamination of the singlet wave function in the broken symmetry solution leading to a larger delocalization of the magnetic orbitals. The hybrid functionals present the same singlet overestimation but to a smaller extent as already noted in ref 1i. All the hybrid functionals gave similar results: the  $J$  values computed with B3LYP and B3PW91 are very close to each other, while smaller  $J$  values are computed with the MPW1PW functional.

From the examination of the data it is clear that DFT predicts the possibility of having a singlet ground state for the model complex. HF theory always gives a triplet as a ground state. It is apparent that the correlation coming from the use of the BS

- (27) Frisch, M. J.; Trucks, G. W.; Schlegel, H. B.; Gill, P. M. W.; Johnson, B. G.; Robb, M. A.; Cheeseman, J. R.; Keith, T. A.; Petersson, G. A.; Montgomery, J. A.; Raghavachari, K.; Al-Laham, M. A.; Zakrewski, V. G.; Ortiz, J. V.; Foresman, J. B.; Cioslowski, J.; Stefanov, B. B.; Nanayakkara, A.; Challacombe, M.; Peng, C. Y.; Ayala, P. Y.; Chen, W.; Wong, M. W.; Andres, J. L.; Replogle, E. S.; Gomperts, R.; Martin, R. L.; Fox, D. J.; Binkley, J. S.; DeFrees, D. J.; Baker, J.; Stewart, J. P.; Head-Gordon, M.; Gonzalez, C.; Pople, J. A. *Gaussian 94*, Revision B.2; Gaussian Inc.: Pittsburgh, PA, 1995.
- (28) *Amsterdam Density Functional (ADF)*, revision 2.3; Scientific Computing and Modelling, Theoretical Chemistry, Vrije Universiteit, Amsterdam, 1997. (a) Baerends, E. J.; Ellis, D. E.; Ros, P. *Chem. Phys.* **1973**, *2*, 42. (b) Boerrigter, P. M.; te Velde, G.; Baerends, E. J. *Int. J. Quantum Chemistry* **1988**, *33*, 87. (c) te Velde, G.; Baerends, E. J. *J. Comput. Phys.* **1992**, *99*, 84. (d) Fonseca Guerra, C.; Visser, O.; Snijders, J. G.; te Velde, G.; Baerends, E. J. In *Methods and Techniques in Computational Chemistry*; Clementi, E., Corongiu, C., Eds.; STEF: Cagliari, 1995; Chapter 8, p 305.
- (29) Vosko, S. H.; Wilk, L.; Nusair, M. *Can. J. Phys.* **1980**, *58*, 1200.
- (30) Becke, A. D. *J. Chem. Phys.* **1993**, *98*, 5648.
- (31) Stephens, P. J.; Devlin, F. J.; Frisch, M. J.; Chabalowski, C. F. *J. Phys. Chem.* **1994**, *98*, 11623.
- (32) (a) Hay, P. J.; Wadt, W. R. *J. Chem. Phys.* **1985**, *82*, 270. (b) Hay, P. J.; Wadt, W. R. *J. Chem. Phys.* **1985**, *82*, 299.
- (33) Stoll, H.; Pavlidou, C. M. E.; Preuss, H. *Theor. Chim. Acta* **1978**, *49*, 143.

- (34) Baker, J.; Scheiner, A.; Andzelm, J. *Chem. Phys. Lett.* **1994**, *216*, 380.

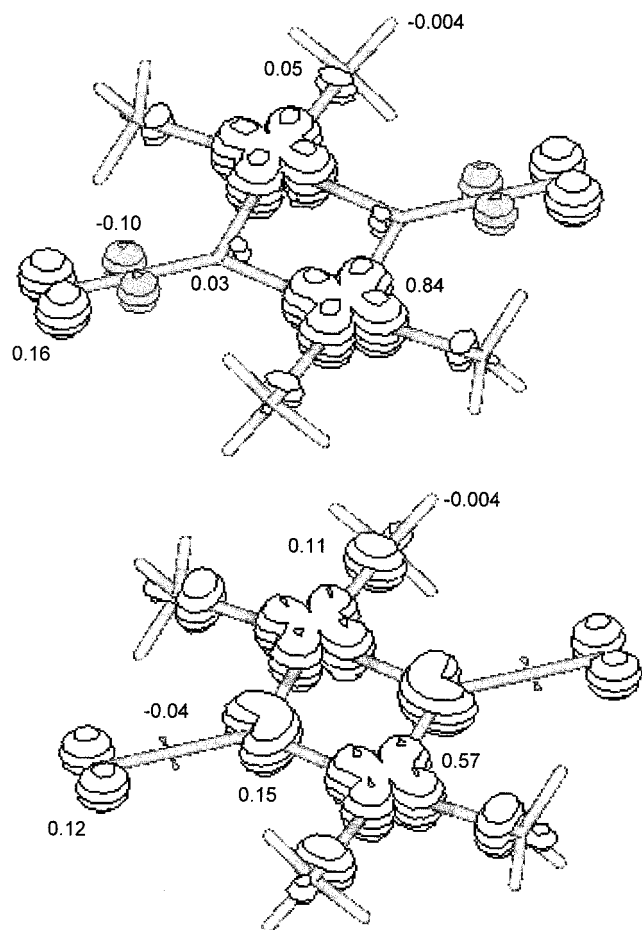


**Figure 4.** Isosurface spin density maps for  $[(\text{NH}_3)_2\text{Cu}(\mu\text{-}1,1\text{-N}_3)_2\text{Cu}(\text{NH}_3)_2]^{2+}$  computed with HF (upper) and DFT-MPW1PW (lower) calculations with  $r = 2.0 \text{ \AA}$ ,  $\varphi = 100^\circ$  on the triplet state. The surfaces are drawn for a value of  $0.01 \text{ e\AA}^{-3}$ . The atomic spin populations obtained through a Mulliken population analysis are also shown.

determinant<sup>10</sup> does not suffice to stabilize the singlet with respect to the triplet state. The DFT results suggest that super-exchange interactions, which are responsible of the dependence of  $J$  on the topology of the complexes, are of importance in determining the overall value of the magnetic coupling constant, in line with the parametrical studies of the exchange interactions in azido-bridged copper(II) dimers by Tuczeck et al.<sup>18,35</sup>

Spin polarization naturally appears in DFT since the open-shell configurations are treated using spin unrestricted calculations. Spin polarization effects are evident when spin densities, computed as the difference between spin-up and spin-down densities, change sign in some region of space and oppose charge delocalization. For example, the spin density arising from a Slater determinant corresponding to a  $M_s = 1$  state of a triplet should be always positive when only charge delocalization is important. Using a single determinant approach, we are only able to compute the gross spin polarization effect, which is the sum of the polarization of all the inner electrons, and we cannot separate the contributions of the individual MO's. However, a look at the spin density maps and at the composition of the magnetic orbitals allows for a qualitative picture of the exchange interactions. The spin density maps corresponding to a value of  $0.01 \text{ e\AA}^{-3}$  computed for  $r = 2.0$  and  $\varphi = 100^\circ$  using unrestricted HF and MPW1PW calculations on the triplet state of  $[(\text{NH}_3)_2\text{Cu}(\mu\text{-}1,1\text{-N}_3)_2\text{Cu}(\text{NH}_3)_2]^{2+}$  are shown in Figure 4.

In Figure 5 the magnetic orbitals obtained from BS calculations at  $\varphi = 100^\circ$  and several  $r$  values are shown. The composition of the magnetic orbitals (Figure 5) gives an idea of the main delocalization of the unpaired electrons and of the super-exchange mechanisms in the active electron approximation.<sup>5</sup> The electrons are mainly localized into an in-plane 3d metal orbital localized on one of the copper atoms with mixing of  $\sigma$  orbitals of the ammonia ligand. No electron delocalization appears on  $\text{N}_2$ , in agreement with the main orbital interaction ( $\pi$  donation) of Schemes 1 and 3. Delocalization of the unpaired electrons is computed on  $\text{N}_1$  and  $\text{N}_3$  and on the other copper(II) center as well. The composition of the magnetic orbitals significantly varies with  $r$ , indicating super-exchange contribution to the magnetic interaction. At the same time, a negative spin density on  $\text{N}_3$  is computed (see Figure 4) which must be ascribed to spin polarization of the doubly occupied molecular orbitals. In the HF calculations (Figure 4, top), this effect is more pronounced. The DFT calculations (Figure 4, bottom), which include correlation, show that a significant spin density is localized on  $\text{N}_1$ , which comes from antibonding interactions with  $\pi$  orbitals and with the inner  $\sigma$  orbitals of  $\text{N}_3^-$ . It is clear that spin polarization is computed to be much smaller than electron delocalization effects. A quantitative comparison with PND data<sup>19</sup> would be helpful to confirm our findings. Unfortunately, PND data are generally interpreted by using a population analysis rather than a direct comparison of density maps. Therefore, the spin populations obtained from a Mulliken population analysis are also shown in Figure 4. The values computed with the MPW1PW functional are in qualitative agreement with the spin populations obtained by the fitting of PND data,<sup>19</sup> which are 0.78, 0.07,  $-0.02$ , and 0.06 for Cu,  $\text{N}_1$ ,  $\text{N}_2$ , and  $\text{N}_3$ , respectively.

From the present calculations, some general considerations can be drawn. (1) A correlation exists between the values of the Cu-N distance,  $r$ , and the Cu-N<sub>1</sub>-Cu, angle,  $\varphi$ , which allows the singlet state to become the ground one. This correlation is less sensitive to the angle  $\varphi$  than that observed in the doubly bridged hydroxo copper(II) systems where change of sign in  $J$  was observed for a variation of only  $2^\circ$  in the bonding angle.<sup>36</sup> (2) The DFT results present a similar qualitative dependence on  $r$  and  $\varphi$  independently of the functional used. The absolute value of  $J$ , however, changes significantly with the form of the functional. (3) The  $J$  and  $J_{\text{cor}}$  values computed using the hybrid functionals generally differ by less than 15%, while in general they are much different when the pure functionals are used. Differences as large as 70% have been computed with the  $X\alpha$  and the VWN functionals. These differences are always bound to values of  $S^2$  for the BS state, much smaller than 1, indicating a stronger contamination of BS from the singlet state which can be properly accounted for only by eq 8. In these cases, the corrections to  $J$  made the triplet state more stable. (4) The  $J$  values computed with the ADF program package are rather close to those computed with the Gaussian basis sets, when analogous functionals are used.

A more careful examination of Table 1 shows that at the point closest to the experimental geometry ( $r = 2.0 \text{ \AA}$ ,  $\varphi = 100^\circ$ ) no functional gives the sign of  $J$  experimentally found. The best agreement with the experimental value is obtained using the hybrid functionals. The MPW1PW functional, with the computed  $J = 44.8 \text{ cm}^{-1}$ , represents the absolute best one. The pure density functionals,  $X\alpha$  and VWN, show an excessive stabiliza-

(35) Tuczeck, F.; Solomon, E. I. *Inorg. Chem.* **1993**, 32, 2850.

(36) Hatfield, W. E. In *Magneto Structural Correlations in Exchange Coupled Systems*; Willett, R. D., Gatteschi, D., Kahn, O., Eds.; NATO Adv. Studies Ser. C; Reidel: Dordrecht, 1985; p 555.

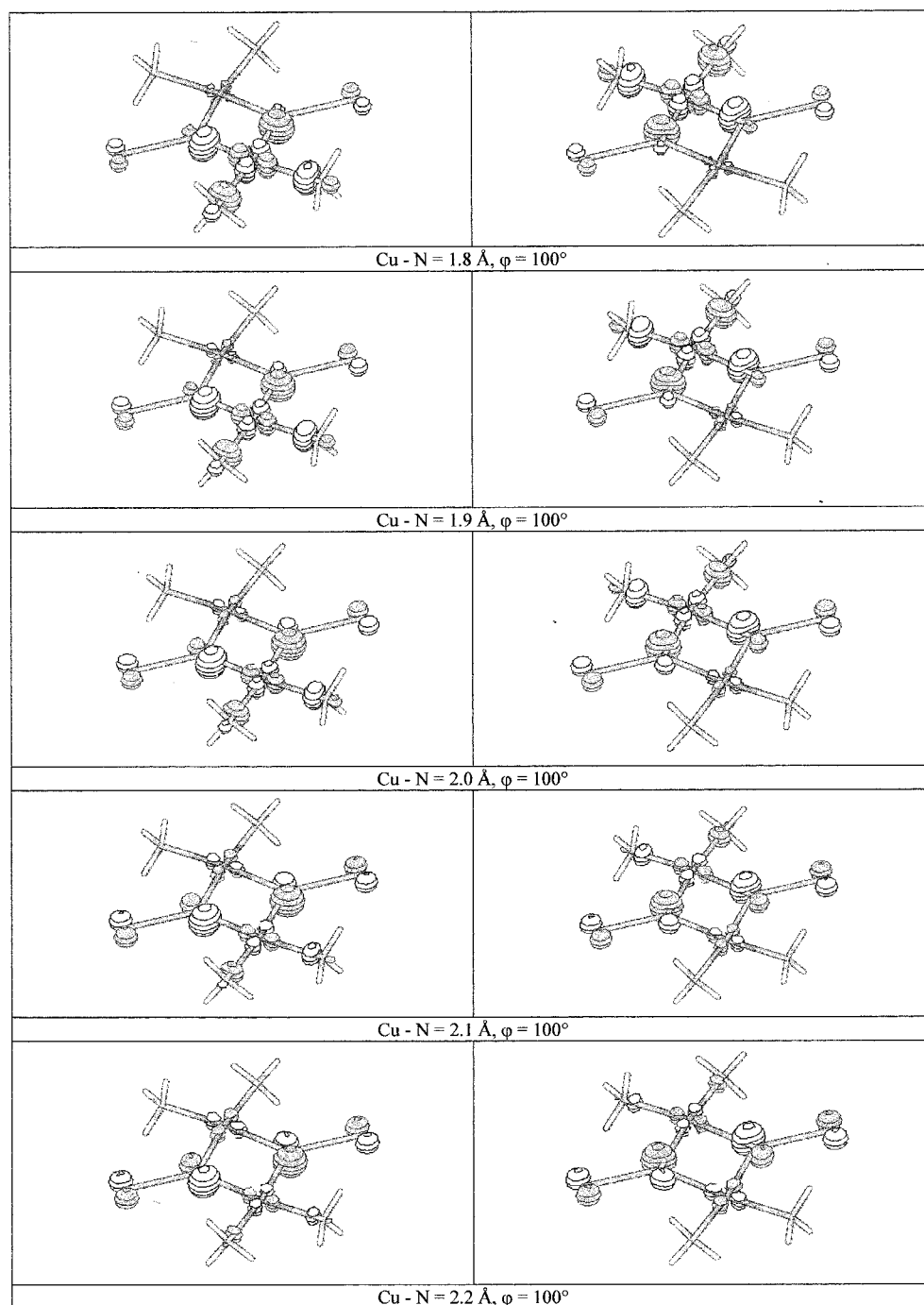


**Figure 5.** Isosurface plots of the magnetic orbitals for  $[(\text{NH}_3)_2\text{Cu}(\mu\text{-}1,1\text{-N}_3)_2\text{Cu}(\text{NH}_3)_2]^{2+}$  computed with DFT-MPW1PW calculations with  $1.8 \leq r \leq 2.0 \text{ \AA}$ ,  $\varphi = 100^\circ$  on the BS state. The surfaces are drawn for a value of 0.01 ( $\text{e}\text{\AA}^{-3}$ )<sup>1/2</sup>.

tion of the singlet state. The HF approach leads to a constantly favored triplet state with respect to the singlet, but the absolute values of the coupling constants are wrong. As already noticed, extensive CI calculations are necessary to lower the energy of the excited singlet state.<sup>17</sup> While the computed dependence of  $J$  on  $r$  and  $\varphi$  is quite similar for all the functionals, the turning point from the ferromagnetic to the antiferromagnetic behavior is not unique; pure density functionals ( $X\alpha$  and VWN) give strong negative  $J$  values for  $r$  values smaller than  $1.9 \text{ \AA}$ , while the hybrid ones give a ferromagnetic ground state already for  $r = 2.0 \text{ \AA}$ . In any case, the ferromagnetic interactions are favored by short  $r$  and small  $\varphi$ . This is pictorially evidenced in Figure 5 where the variation of the composition of the magnetic orbitals on  $r$  is shown. The solutions corresponding to larger  $r$

are more delocalized, and consequently, the overlap between the magnetic orbitals, which favors the antiferromagnetic interaction in the active electron approximation of the exchange interaction,<sup>5</sup> is larger. It should be noted that a decrease of  $J$  is observed on passing from **2** to **1** (Scheme 1), which can be ascribed to a lengthening of the Cu-N bond and to the larger Cu-N<sub>1</sub>-Cu angle observed in the crystal structure.<sup>16</sup>

$J$  values comparable with the experimental data have been obtained with  $r = 1.9 \text{ \AA}$  and  $\varphi$  between  $100^\circ$  and  $106^\circ$  (see Table 1) using the MPW1PW functional. Also, the B3LYP and B3PW91 functionals give, however, values close to the experiment in the same angular range. A complete agreement with the experiment, using the experimental  $r$  and  $\varphi$  values, cannot be expected since we are using model systems in order to



**Table 2.** Geometry Optimization of  $[(\text{NH}_3)_2\text{Cu}(\mu\text{-}1,1\text{-N}_3)_2\text{Cu}(\text{NH}_3)_2]^{2+}$ 

	exptl value <sup>a</sup>	optimized value <sup>b</sup>
Cu–N	1.99	2.000
Cu–NH <sub>3</sub>	2.00	2.050
N <sub>1</sub> –N <sub>2</sub>	1.18	1.251
N <sub>2</sub> –N <sub>3</sub>	1.11	1.165
H <sub>3</sub> N–Cu–NH <sub>3</sub>	94°	93.8°
Cu–N <sub>1</sub> –Cu	100.5°	102.8°

<sup>a</sup> From the X-ray crystal structure<sup>15</sup> of  $[\text{Cu}_2(\text{tbupy})_4(\text{N}_3)_2](\text{ClO}_4)_2$ .

<sup>b</sup> The optimization was performed using DFT with the MPW1PW functional on the  $S = 1$  spin state in  $D_{2h}$  symmetry.

achieve results at reasonable computational expenses. Furthermore, using the real structure, any symmetry element is removed and low symmetry mixing complicates the analysis of the composition of the molecular orbitals. These facts pushed us to look for magnetostructural correlations rather than for the reproduction of the experimental value. In order, however, to understand which factors can lead to a computed  $J$  value closer to the experimental findings, we have performed additional calculations using the DFT approach with the MPW1PW functional. First of all, the model structure was fully optimized. Since the singlet state cannot be described with one single Slater determinant, geometry optimization of the  $[(\text{NH}_3)_2\text{Cu}(\mu\text{-}1,1\text{-N}_3)_2\text{Cu}(\text{NH}_3)_2]^{2+}$  complex was performed on the triplet state. The computed geometry is compared to the experimental one in Table 2. The computed bond distances are longer than the experimental ones. The largest deviation, 0.07 Å, is computed in the bond distance N<sub>1</sub> – N<sub>2</sub>. The Cu–N<sub>1</sub>–Cu bond angle is computed at 102.8°, and the corresponding  $J$  value is  $J_{\text{cor}} = 506.1 \text{ cm}^{-1}$ . A large antiferromagnetic interaction is still computed.

A structural deformation present in  $[\text{Cu}_2(\text{tbupy})_4(\text{N}_3)_2](\text{ClO}_4)_2$  which we have not yet considered in our model molecule is the deviation of the nitrogen atoms of N<sub>3</sub><sup>–</sup> from the  $xy$  plane of Figure 1. This reduces the overall symmetry of the molecule to  $C_1$ . Using the experimental values  $r = 2.0 \text{ Å}$  and  $\varphi = 100^\circ$ , we have performed the calculation of  $J$  by moving in the trans fashion the nitrogen atoms of N<sub>3</sub><sup>–</sup> 16° from the  $xy$  plane, like in the experimental structure. The computed  $J_{\text{cor}}$  value reduces from 44.8 to 12.8 cm<sup>–1</sup> in the model with NH<sub>3</sub> groups.

In the final calculations, we have used the coordinates observed in the crystal structure<sup>16</sup> of  $[\text{Cu}_2(\text{tbupy})_4(\text{N}_3)_2](\text{ClO}_4)_2$  except for the *tert*-butyl groups which were replaced by hydrogen atoms. The computed  $J_{\text{cor}}$  value is  $-106.1 \text{ cm}^{-1}$  in remarkably good agreement with the experimental<sup>16</sup> value ( $J = -105(25) \text{ cm}^{-1}$ ). The spin populations computed for Cu and the N atoms of the azido groups (averaged for the small anisotropy introduced by the symmetry lowering) are 0.56, 0.15,  $-0.04$ , and 0.12, in close agreement with the values computed on the model  $[(\text{NH}_3)_2\text{Cu}(\mu\text{-}1,1\text{-N}_3)_2\text{Cu}(\text{NH}_3)_2]^{2+}$  cation. It is reasonable to think that  $\pi$  effects of pyridine and the symmetry lowering, which cause a mixing of orthogonal 3d orbitals in

the ground state, are responsible for the strong variation of  $J_{\text{cor}}$  on passing from the symmetric model to the real molecule. The low-symmetry effects are also apparent from the variation of  $J_{\text{cor}}$  on passing to the asymmetric model, which lowers  $J_{\text{cor}}$  to 12.8 cm<sup>–1</sup> in the model with NH<sub>3</sub> groups.

## Conclusions

In this paper we have addressed several points which are currently encountered when trying to correlate observed magnetic properties to the structure of the paramagnetic molecules using DFT calculations. A fast and efficient spin projection technique is presented, which allows a better projection of the singlet state from the BS determinant.

The use of model molecules in the calculations was found to give  $J$  values that can differ in magnitude from the experimental findings. The present results shows that only using pyridine as the terminal ligand, which still constitutes a modelization for the *tert*-butylpyridine, we can compute a  $J$  value close to the experimental one. Also small geometrical deformations can influence the actual value of  $J$ . The deviation of the N<sub>3</sub><sup>–</sup> groups from the  $xy$  plane of only 16° changes the computed  $J$  value from 44.8 to 12.8 cm<sup>–1</sup>. For these reasons also, the geometry optimization of the molecule performed in the gas phase can hardly give structures which afford  $J$  values comparable with the experimental data, which are generally measured in the solid state. Environmental effects are in general responsible for small deformations of the molecules in the solid, which can strongly influence the observed  $J$  values. All of the above findings can therefore be considered when choosing the proper functional to perform the calculations. Only the overall variation of  $J$  with the geometrical parameters was found to be rather independent of the actual form of the functional, with the computed values differing from one functional to the other.

The main question to ask is can DFT be used to compute and predict the magnetic behavior of binuclear systems? The calculation of  $J$  performed at the experimental geometry is in good agreement with the observed one, using the hybrid functional MPW1PW. Also magnetostructural correlations can be done with at least a semiquantitative agreement. The local functionals give always the singlet state more contaminated by the excited ones and lead to larger antiferromagnetic  $J$  values. The exchange coupling constants computed with the hybrid methods were found to be less affected by the particular form of the functionals. The present calculations have shown that an antiferromagnetic azido-bridged dimer can be expected. Testing this result experimentally can yield more hints to the previous question, which is of fundamental importance in molecular magnetism.

The combined use of spin density maps and of magnetic orbitals representation can be used to qualitatively understand the competitive role of spin delocalization and super-exchange interactions in determining the final  $J$  values.